

Noname manuscript No. (will be inserted by the editor)
--

Radial Basis Functions Application for Multi-level Vector Field Approximation

Michal Smolik · Vaclav Skala

Received: 20.2.2019 / Accepted: date

Abstract We propose a new approach for meshless multi-level radial basis function (ML-RBF) approximation which offers data sensitive compression and progressive details visualization. It leads to an analytical description of compressed vector fields, too. The proposed approach approximates the vector field in multiple levels of details. The low level approximation removes minor flow patterns while the global character of the flow remains unchanged. And conversely, the higher level approximation contains all small details of the vector field. The ML-RBF has been tested with a numerical forecast data set to prove its ability to handle data with complex topology. Comparison with the Fourier vector field approximation has been made and significant advantages, i.e. high compression ratio, accuracy, extensibility to a higher dimension etc., of the proposed ML-RBF were proved.

Keywords Radial basis functions · adaptive shape parameter · vector field · approximation · Gaussian low-pass filter · Fourier transform

1 Introduction

In applied sciences, interpolation and approximation are probably the most frequent techniques used [8]. In this paper, we propose a new approach for meshless multi-level radial basis function (ML-RBF) approximation which offers data sensitive compression, progressive details visualization and leads to analytical description of compressed vector fields. It is capable to handle vector data fields with complex topology as well.

M. Smolik
Faculty of Applied Sciences, University of West Bohemia, Plzen, Czech Republic
E-mail: smolik@kiv.zcu.cz

V. Skala
Faculty of Applied Sciences, University of West Bohemia, Plzen, Czech Republic
E-mail: skala@kiv.zcu.cz

A vector field is a function that assigns to each point a vector. Vector fields come mostly from numerical simulations, i.e. Computational Fluid Dynamics (CFD) [17], [18], [1] and Finite Element Method (FEM) [29], [6]. The analysis of the vector field can be done at any location of the vector field [15], [46], [42]. However the most important places of the vector field are so-called critical points [15].

Topology-based flow visualization is well known technique [22]. However, the result can be a cluttered image which is difficult to interpret, when the topology-based technique is used in complex and information-rich data sets. One solution of this problem is described in the paper [47], which optimizes the topology. The Multi-level topology visualization of vector field data sets is presented in [25]. The algorithm visualizes the topology without excessive cluttering while maintaining the global structure of the flow. Another approach [4] uses fully adaptive multiresolution schemes for strongly degenerate parabolic equations with discontinuous flux. The paper [50] uses a multi-scale model for solute transport in a wavy-walled channel. This approach concerns steady flow and identifies conditions under which is the approximation uniformly valid in a full channel flow. The paper [39] simplifies the vector field using the reduction of critical points according to a quantitative measure of their stability, which is computed as the minimum amount of vector field perturbation that is required to remove the critical point. This leads to a hierarchical simplification scheme that encodes flow magnitude in its perturbation metric. A topological denoising technique based on a global energy optimization is proposed in [14], which allows the topology-controlled denoising of scalar fields. The algorithm for topology-controlled denoising of scalar fields, which processes small patches of the domain independently, is presented in [14]. It is based on a global energy optimization and avoids the introduction of new critical points. The paper [5] describes a numerical comparison between RBF local and global methods and highlights the possible advantage of using local methods for the approximation of vector fields. The vector field approximation for two-dimensional vector fields that preserves their topology and significantly reduces the memory footprint is presented in [21]. This approximation is based on a segmentation and the flow within each segmentation region is approximated by an affine linear function. The paper [24] reduces the size degree of the complexity of density variations. This approach is compared with a phase-field method [20].

The Fourier transform decomposes a function into the frequencies that make it up. It can be used for vector field analysis and approximation or simplification. The Clifford Fourier transform in [9] allows a frequency analysis of vector fields and the behavior of vector-valued filters. In frequency space, vectors are transformed into general multivectors of the Clifford Algebra. Many basic vector-valued patterns, such as source, sink, saddle points, and potential vortices, can be described by a few multivectors in frequency space. A two-dimensional filtering operation, involving both curl and divergence, is applied in [28] to the $2D$ Clifford Fourier Transform in order to simultaneously enhance important features of a $2D$ vector field, such as vortices and pairs of sources and sinks. The approach [32] defines convolution operators on vector

fields using geometric algebra. This includes a corresponding Clifford Fourier transform of a spatial vector or multivector data. This approach is used for the analysis of the fluid flow. There are also different approaches to transforming vector-valued data using a Fourier transform [3], [16] and [10].

The proposed (ML-RBF) vector field approximation method has variety of uses. The vector field data sets come mostly from the numerical simulations and contains very large number of sample points, i.e. the data set is very large. This data sets need to be stored for future use and backup. Thus, the approximation techniques are used to compress the vector field data sets. For this reason, we propose a new technique for vector field ML-RBF approximation. The ML-RBF technique is suitable for fast preview of the vector field data set as visualization can be done using only first level of details or few first levels of details. This is also useful for mobile devices as the data set does not need to be transferred whole at once and the data transfer can be reduced to only first level of details. The additional levels of details can be transferred additionally; one by one when they are needed. Another use of the proposed ML-RBF vector field approximation is the exploration and the insight of the vector field as the vector field is visualized without excessive cluttering while maintaining the global structure of the vector field. Next, the compressed vector field is in the form of an analytical description which can be used for further vector field analysis and symbolic manipulation.

2 Radial Basis Functions

Radial basis function (RBF) is a real-valued function whose value depends only on some distances. i.e. the RBF interpolation [30] and approximation [11], [35], [45] of scattered data is invariant under all Euclidean transformations. The RBF interpolation and approximation is widely used in many scientific disciplines, e.g. for solution of partial differential equations [23], [52], image reconstruction [48], neural networks [19], [13], [51], GIS systems [26], optics [31], vector fields approximation [44], [43], [40], [41], etc.

The RBF interpolation or approximation leads to a system of linear equations $\mathbf{Ax} = \mathbf{b}$ which is to be solved. It should be noted, that if the RBF is used for interpolation or approximation of data with large span, additional numerical problems can be expected [36], [38], [37].

There exist two groups of radial basis functions according to their influence. The first group are “global” RBFs [34]. The second group are “local” RBFs. Application of global RBFs usually leads to ill-conditioned system, especially

in the case of large data sets with a large span [27], [38]. The following global RBFs will be used in our experiments:

$$\begin{aligned}
 \text{Thin Plate Spline (TPS)} \quad \varphi_1(r) &= r^2 \log r \\
 \text{Gauss function} \quad \varphi_2(r) &= e^{-(\epsilon r)^2} \\
 \text{Inverse Quadric (IQ)} \quad \varphi_3(r) &= \frac{1}{1 + (\epsilon r)^2} \\
 \text{Inverse Multiquadric (IMQ)} \quad \varphi_4(r) &= \frac{1}{\sqrt{1 + (\epsilon r)^2}} \\
 \text{Multiquadric (MQ)} \quad \varphi_5(r) &= \sqrt{1 + (\epsilon r)^2}
 \end{aligned} \tag{1}$$

“Local” RBFs were introduced in [49] as compactly supported RBF (CSRBF). They satisfy the following condition:

$$\begin{aligned}
 \varphi(r) &= (1 - r)_+^q P(r) \\
 &= \begin{cases} (1 - r)^q P(r) & 0 \leq r \leq 1 \\ 0 & r > 1 \end{cases}
 \end{aligned} \tag{2}$$

where $P(r)$ is a polynomial function and q is a parameter. The following local RBFs will be used in our experiments:

$$\begin{aligned}
 \varphi_6(r) &= (1 - r)_+ \\
 \varphi_7(r) &= (1 - r)_+^3 (3r + 1) \\
 \varphi_8(r) &= (1 - r)_+^5 (8r^2 + 5r + 1) \\
 \varphi_9(r) &= (1 - r)_+^2 \\
 \varphi_{10}(r) &= (1 - r)_+^4 (4r + 1) \\
 \varphi_{11}(r) &= (1 - r)_+^6 (35r^2 + 18r + 3) \\
 \varphi_{12}(r) &= (1 - r)_+^8 (32r^3 + 25r^2 + 8r + 1)
 \end{aligned} \tag{3}$$

3 Proposed approach

In this section we describe our new proposed approach for multi-level vector field approximation using radial basis functions. The algorithm is composed by three main steps. The first step is the calculation of approximation error, the second one is the use of a Gaussian low-pass filter and the last one is the approximation using RBF. The pseudo-code of the proposed approach is in Algorithm 1. The algorithm is iterative and runs until the maximum level of details is computed.

In the following, we describe the proposed method on a $2D$ vector field. However, this algorithm is easy to extend to higher dimensions.

Algorithm 1 The multi-level RBF approximation of vector field.

```

1: vectorField  $\mathbf{v} = [\mathbf{v}_x, \mathbf{v}_y] = [\mathbf{0}, \mathbf{0}]$  ▷ Initialization
2:  $\sigma =$  initial value ▷ Standard deviation
3: procedure MULTI-LEVELRBF(Flow  $\bar{\mathbf{v}} = [\bar{\mathbf{v}}_x, \bar{\mathbf{v}}_y]$ )
4:   for  $i \leftarrow 1, LevelCount$  do
5:      $\mathbf{Err} = \bar{\mathbf{v}} - \mathbf{v}$ ; ▷ Error estimation
6:      $\mathbf{Err} = Gauss(\mathbf{Err}, \sigma)$  ▷ Gaussian low-pass filter
7:      $\mathbf{e} =$  Find extrema of  $\mathbf{Err}$ 
8:      $\mathbf{x}_0 =$  Find critical points of  $\mathbf{Err} + \mathbf{v}$ 
9:      $RBF =$  RBF approximation ( $\mathbf{e}, \mathbf{x}_0, \mathbf{Err}$ )
10:     $\mathbf{v} += RBF$  ▷ Update vector field
11:     $\sigma /= 2$  ▷ Decrease  $\sigma$ 
12:   end for
    
```

The first step of the proposed method is the error estimation. We need to compute the error for both components of a vector field

$$\begin{aligned} \mathbf{Err}_x &= \bar{\mathbf{v}}_x - \mathbf{v}_x, \\ \mathbf{Err}_y &= \bar{\mathbf{v}}_y - \mathbf{v}_y, \end{aligned} \quad (4)$$

where \mathbf{Err}_x and \mathbf{Err}_y are error vectors, $\bar{\mathbf{v}}_x$ and $\bar{\mathbf{v}}_y$ are the x and y components of input flow field vectors, \mathbf{v}_x and \mathbf{v}_y are the x and y components of actual flow field approximation vectors. For the 0 (zero) level vector field approximation, $\mathbf{v}_x = \mathbf{0}$ and $\mathbf{v}_y = \mathbf{0}$.

Vector fields can be very complex data sets with very large number of critical points. The multi-level RBF vector field approximation aims to approximate vector field in several levels of details. The lowest level of details should describe only the main global character of the flow. Each additional level of details should add some more details into the approximation. Thus with higher levels of details, the approximated vector field will contain more and more critical points and smaller flow details as well.

The next step of the proposed multi-level RBF vector field approximation is filtering the data set to obtain a simplified one. In our case, we filter the $2\frac{1}{2}D$ error data from (4), i.e. $2D$ function with associated errors. The low-pass Gaussian filter is used to filter the $2\frac{1}{2}D$ data. The Gaussian filter can have different scope and thus filter either small perturbations of the flow or large changes of the flow. The Gaussian filter has the formula

$$G(x, y) = \frac{1}{2\pi\sigma^2}g(x, y), \quad (5)$$

where x and y are the location coordinates, σ is the standard deviation of the Gaussian distribution and $g(x, y)$ is defined as

$$g(x, y) = e^{-\frac{x^2+y^2}{2\sigma^2}}. \quad (6)$$

For each level of approximation, a different value of σ is to be chosen. For the first level of approximation we need to set up the initial value of σ . The

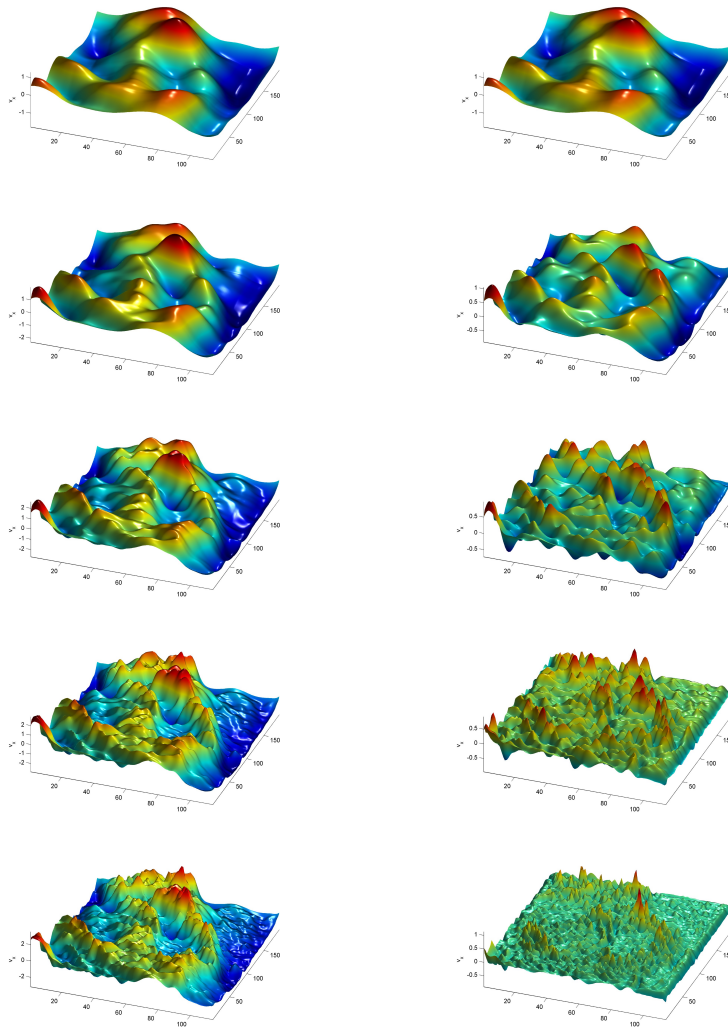


Fig. 1 The right column represents Err_x of a vector field for different levels of details, i.e. from top to bottom: $\sigma = 10, 5, 2.5, 1.25$ and 0.625 . The left column represents the v_x component of a vector field for different levels of details, i.e. v_x is the sum of Err_x from the previous levels of details.

value of σ in every following level will always be half of the value σ from the previous level. The initial value of standard deviation, i.e. σ_1 , can be selected as

$$\sigma_1 = s_\sigma \cdot MIN(x_{min} - x_{max}, y_{min} - y_{max}), \quad (7)$$

where x_{min} , x_{max} , y_{min} , y_{max} are minimal and maximal values of x and y coordinates, and s_σ is a constant reflecting the data size and sampling density. A pragmatical choice is $s_\sigma = \frac{1}{10}$. If this value s_σ is smaller, then the first level

vector field approximation will be even more simplified, and conversely. An example of an application of a Gaussian low-pass filter on a vector field data set¹ [7] is in Fig. 1.

The next step of the proposed method is the RBF approximation, for which we need the locations of radial basis functions, i.e. the centers. The centers need to be in the location of critical points, i.e.

$$\mathbf{x}_0 = \text{Find_critical_points}(\mathbf{Err} + \mathbf{v}). \quad (8)$$

Moreover at the extremes of \mathbf{v}_x , resp. \mathbf{v}_y , are located the additional centers of radial basis functions. The number of extremes will increase with increasing the level of approximation.

The radial basis function used for the RBF approximation is $\varphi_{10}(r)$ and it was used to demonstrate the proposed approach. It was selected due to continuity properties, computational complexity and it is the most adequate radial basis function according the tests in chapter 5.1. The RBF function $\varphi_{10}(r)$ is defined as

$$\varphi(r)_{10} = (1 - \epsilon r)_+^4 (4\epsilon r + 1), \quad (9)$$

where ϵ is the shape parameter of the radial basis function. The shape parameter is different for every level of approximation to capture different levels of details of the vector field. The shape parameter should be selected in a way that (9) has a similar shape as the Gaussian filter (6), i.e. the absolute difference of these two functions is minimal. We performed tests to select the best shape parameter, see Fig. 6 in ‘‘Results’’ section. For different standard deviations σ in (6), the best shape parameter is

$$\epsilon = \frac{0.2694}{\sigma}. \quad (10)$$

Now, we can compute the RBF approximation for each x and y component separately. To approximate \mathbf{Err}_x , the centers of radial basis functions will be locations of critical points from (8) and extremes of \mathbf{Err}_x , similarly for \mathbf{Err}_y .

After the RBF approximation, we need to update the actual level vector field

$$\begin{aligned} \mathbf{v}_x &= \mathbf{v}_x + \mathbf{RBF}_x, \\ \mathbf{v}_y &= \mathbf{v}_y + \mathbf{RBF}_y, \end{aligned} \quad (11)$$

The algorithm is repeated until the required number of levels of details is reached. With every additional level of details, the vector field RBF approximation is more accurate.

In the following chapter experimental results of the proposed multi-level RBF method are presented.

¹ Data set of wind flow at a height of 10m over the surface of the Czech Republic courtesy of the Institute of Computer Science of the Czech Academy of Sciences.

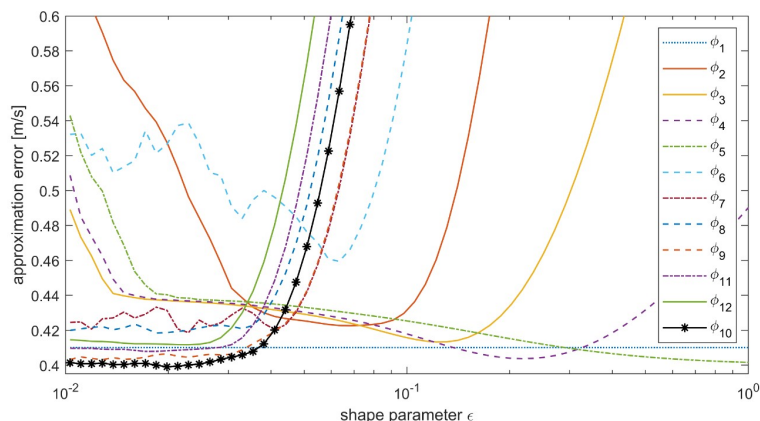


Fig. 2 Approximation errors for different shape parameters.

4 Results

The multi-level RBF (ML-RMB) vector field approximation is especially convenient for visualization purposes and vector field data understanding. The numerical forecast data set taken from [7] was used to prove the multi-level RBF approximation properties and for comparison with approximation based on the Fourier transform. The data set consists of around $2.2 \cdot 10^4$ points.

4.1 Selection of the RBF

One of the most important and critical part in the RBF approximation is the selection of the most adequate radial basis function [33], [27]. We tested the radial basis functions in (1) and (3). We selected around 275 centers of RBF, so that the compression ratio of the RBF approximation is 80 : 1. For each RBF in (1) and (3) we tested the approximation error for different shape parameters. The approximation error is computed using (16) and the results are presented in Fig. 2. It can be seen that the “local” RBFs have all similar behavior and the approximation error is low when using lower values of shape parameter. In our case, we select a local RBF function, as the approximation matrix will be sparse and better conditioned. Also we will be able to approximate larger data sets compared to the case, when using “global” RBFs which leads to ill-conditioned full matrices, in general. The best choice according to the results in Fig. 2 is the radial basis function $\varphi_{10}(r)$ as it has the lowest approximation error and is C_2 continuous.

We also compared the selected RBF $\varphi_{10}(r)$ with other RBFs and computed the difference histogram of approximation error, see Fig. 3. The test was performed always for the best shape parameter for each RBF. The positive values for small approximation errors mean that the approximation with the selected

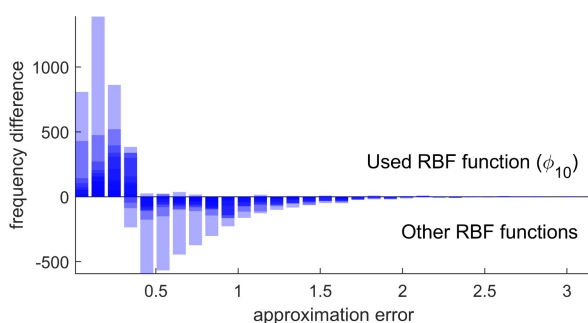


Fig. 3 Difference histograms of approximation errors. All difference histograms are blended over each other.

RBF has much more smaller approximation errors. The negative values for larger approximation errors mean that the approximation with the selected RBF has much less larger approximation errors. This test clearly confirmed the selection of $\varphi_{10}(r)$ as the most adequate RBF for our proposed approach.

4.2 Multi-level RBF Approximation

To compute the RBF approximation, we need to find the centers of radial basis functions for every level of details. We tested the number of centers and summarized this in Table 1.

Table 1 The number of centers for RBF approximation at every added level of details.

Level number	σ	# of extreme points in v_x	# of extreme points in v_y	# of critical points
1	10	28	27	2
2	5	58	54	2
3	2.5	161	176	10
4	1.25	517	539	25
5	0.625	1238	1249	49

It can be seen that even when computation is done until the last level of details, we need for x and y components of the vector field approximately $2.1 \cdot 10^3$ centers of radial basis functions. This is approximately 9.5% of the input data set and the resulting vector field approximation is very similar to the original one.

At each level of RBF approximation, we approximate the $2\frac{1}{2}D$ functions Err_x and Err_y , see Fig. 4a,d,g,j,m for Err_x and Fig. 5a,d,g,j,m for Err_y . To find the location of radial basis functions, we use a Gauss filter for smoothing and then locate extremes of the resulting $2\frac{1}{2}D$ function, see Fig. 4b,e,h,k,n for Err_x smoothing and Fig. 5b,e,h,k,n for Err_y smoothing. These $2\frac{1}{2}D$ functions

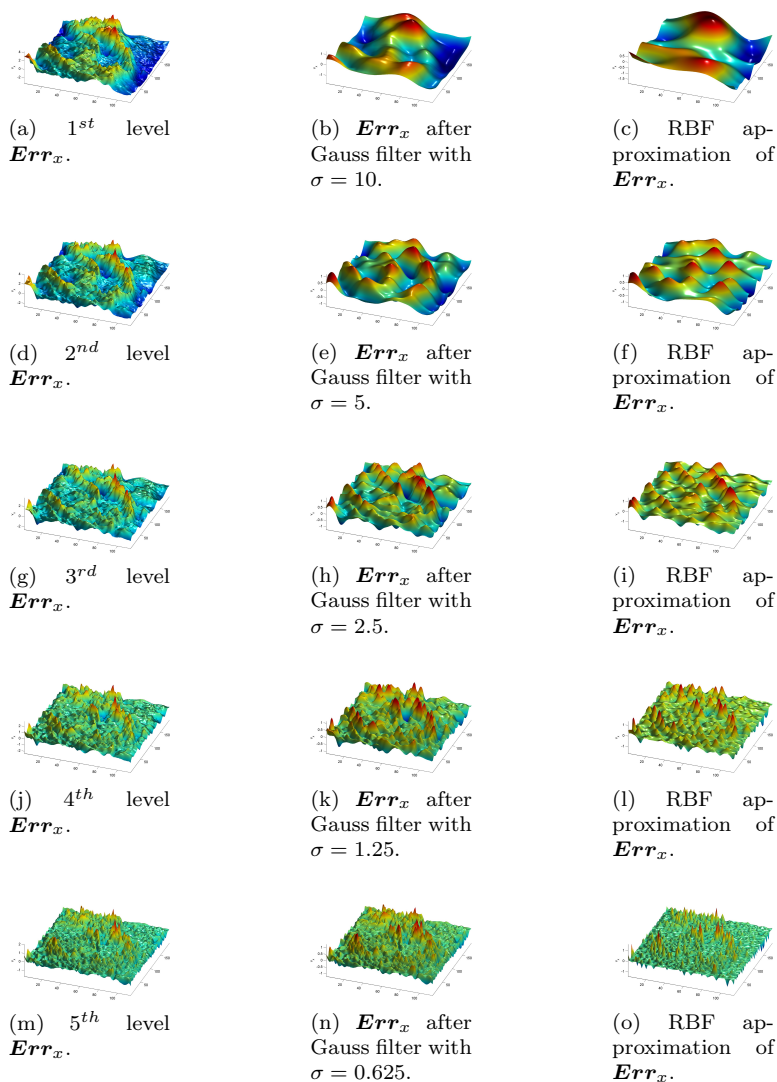


Fig. 4 Err_x function for each level of details, filtered Err_x functions and the RBF approximation of Err_x .

have the same global character as the original $2\frac{1}{2}D$ functions Err_x and Err_y , but they do not contain tiny details.

The shape parameter is different for every level of approximation to capture different levels of details of the vector field. The shape parameter should be selected in a way that (9) has a similar shape as the Gaussian filter (6), i.e. the absolute difference of these two functions is minimal. We performed tests

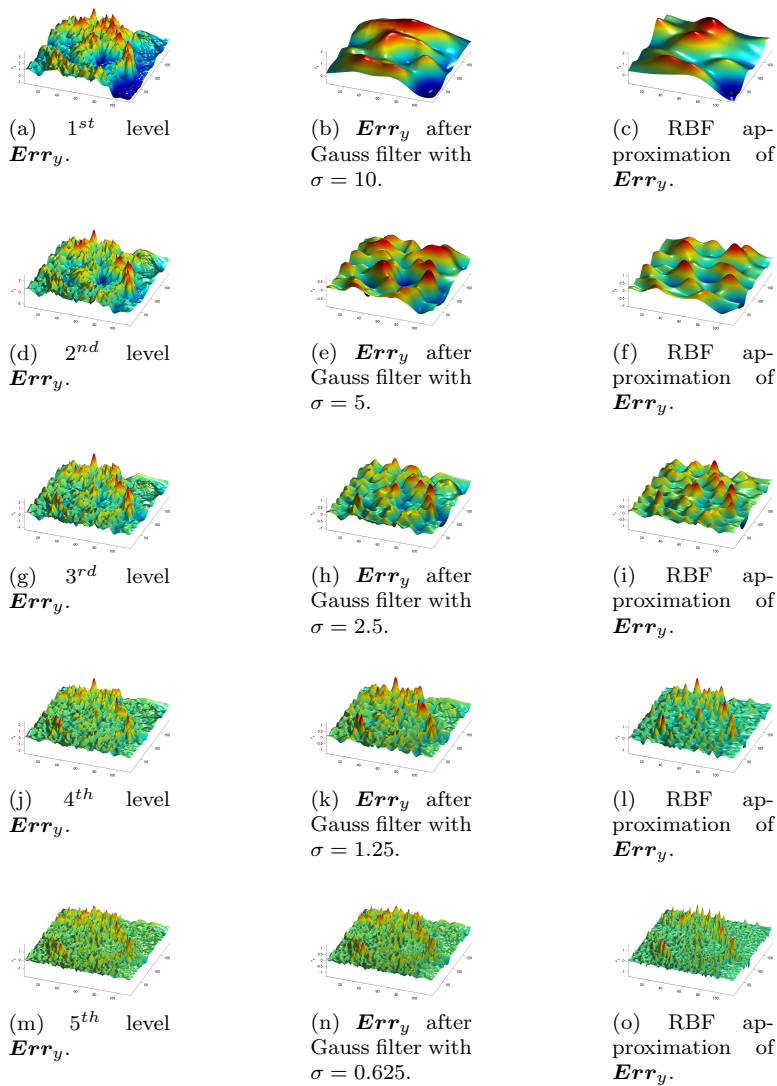


Fig. 5 Err_y function for each level of details, filtered Err_y functions and the RBF approximation of Err_y .

to select the best shape parameter. The results in Fig. 6 are for a Gaussian filter with $\sigma = 1$.

The best shape parameter is $\epsilon = 0.2694$, see Fig. 6. For different standard deviations σ , the best shape parameter is

$$\epsilon = \frac{0.2694}{\sigma}. \quad (12)$$

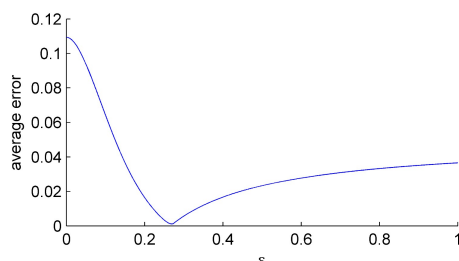


Fig. 6 The average absolute difference of (5) with $\sigma = 1$ and (9) for different values of shape parameter ϵ and $r \in [0; 1/\epsilon)$.

The RBF approximations of \mathbf{Err}_x are in Fig. 4c,f,i,l,o and approximations of \mathbf{Err}_y are in Fig. 5c,f,i,l,o. The RBF approximations of \mathbf{Err}_x and \mathbf{Err}_y are very close to the filtered $2\frac{1}{2}D$ functions of \mathbf{Err}_x and \mathbf{Err}_y , as the placement of radial basis function centers and the shape parameter of radial basis functions are very well chosen.

The resulting multi-level RBF approximation of the vector field is visualized in Fig. 7. It can be seen that with every additional level of details the approximated vector field is closer to the original one. Even the first level approximation has the same global characteristics as the original vector field.

To measure the quality of the vector field approximation, we compute the approximation error at every point of the vector field using the following formula

$$error^{(i)} = \sqrt{\left(v_x^{(i)} - \bar{v}_x^{(i)}\right)^2 + \left(v_y^{(i)} - \bar{v}_y^{(i)}\right)^2}, \quad (13)$$

where $v_x^{(i)}$ and $v_y^{(i)}$ are approximated values, $\bar{v}_x^{(i)}$ and $\bar{v}_y^{(i)}$ are the original values of the vector field and $error^{(i)}$ is the approximation error at the i^{th} point. The approximation error is color-coded in Fig. 8. It can be seen that the approximation error is lower with every additional level of details.

4.3 Comparison With Existing Approach

The proposed approach needs to be compared with an other existing approach. We selected the mostly used Fourier transform [12], [2]. The vector field is approximated with the Fourier transform using the following formula

$$F(\alpha, \beta) = \int_{-\infty}^{\infty} \int_{-\infty}^{\infty} v(x, y) e^{-2\pi i(x\alpha + y\beta)} dx dy, \quad (14)$$

where α and β are frequencies (see Fig. 9). According to the required accuracy, only some of the most important frequencies are selected to approximate the vector field. This approximated vector field represented by a list o frequencies

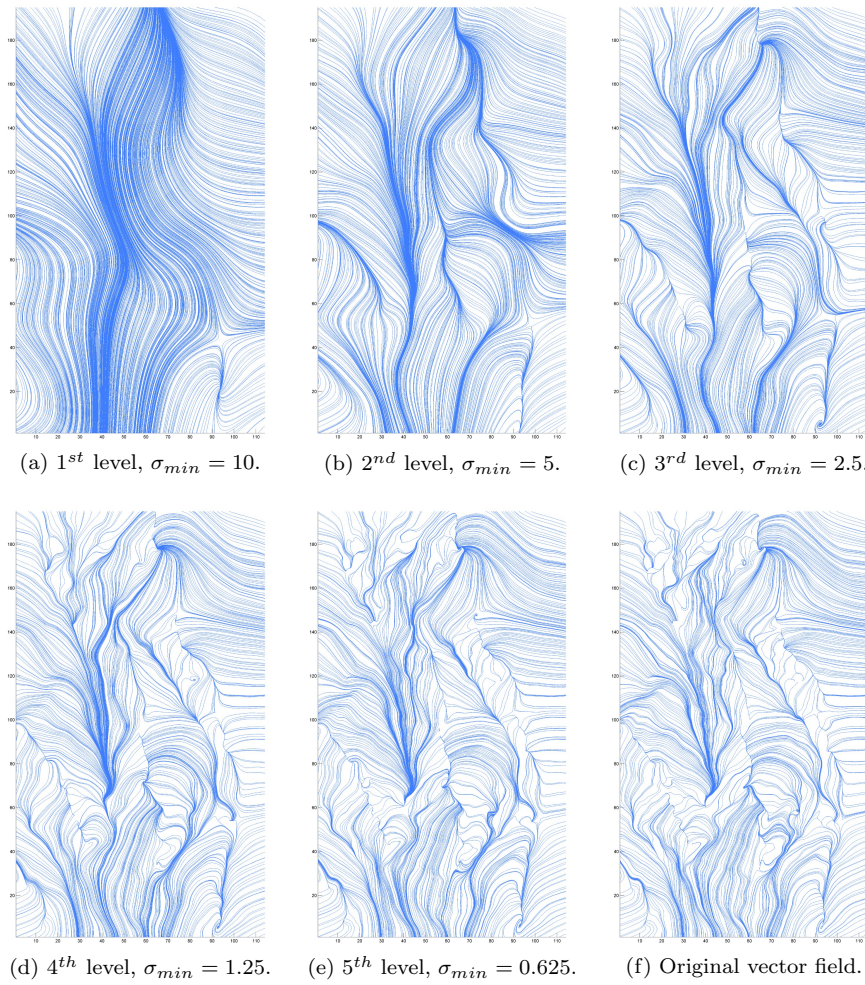


Fig. 7 The vector field approximation for different levels of details (a-e) and the original vector field (f).

can be transformed back to the vector field using the following inverse Fourier transform

$$v(x, y) = \frac{1}{(2\pi)^2} \int_{-\infty}^{\infty} \int_{-\infty}^{\infty} F(\alpha, \beta) e^{2\pi i(x\alpha + y\beta)} d\alpha d\beta. \quad (15)$$

To compare the proposed approach for multi-level vector field approximation with the Fourier transform vector field approximation, we need to compute and compare the vector field approximation errors. We can compute the average difference approximation error using the following formula

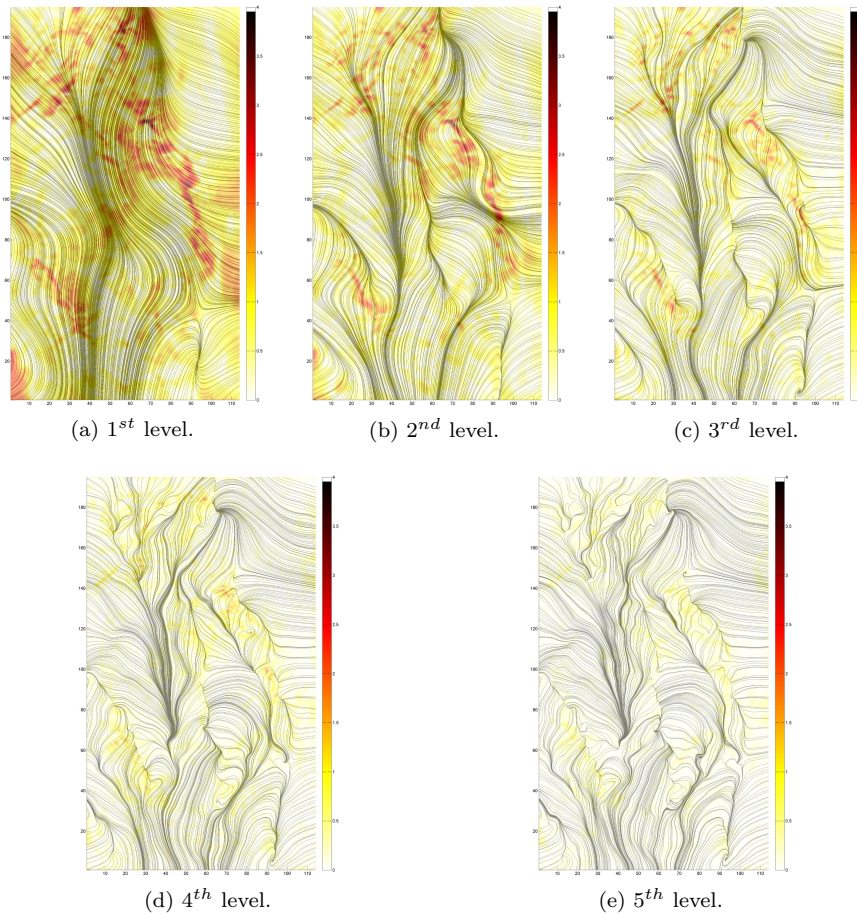


Fig. 8 The vector field approximation error for different levels of details. The approximation error is computed using (13). All color bars have the same error range for better comparison.

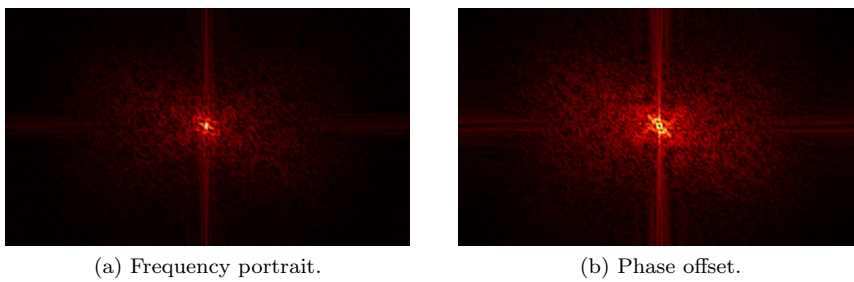
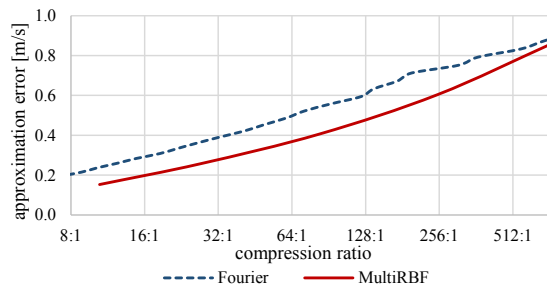
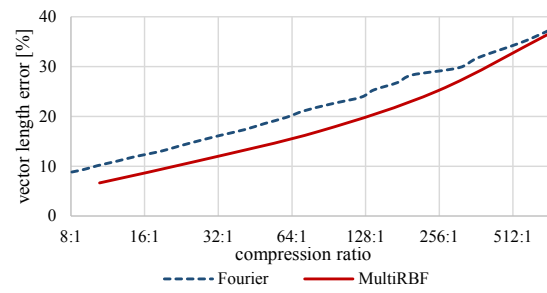


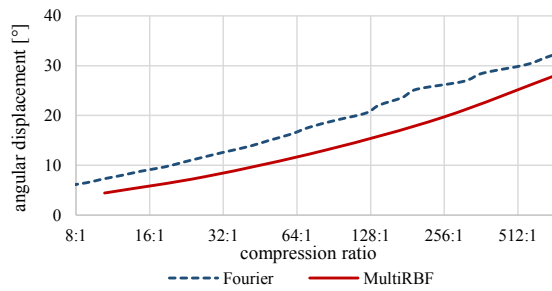
Fig. 9 Approximation of the vector field using Fourier transform.



(a) The average difference approximation error.



(b) The average vector length error.

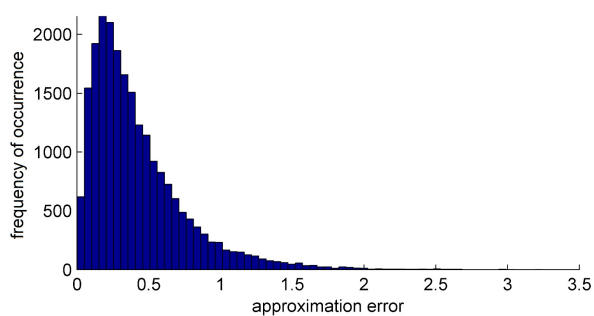


(c) The average angular displacement error.

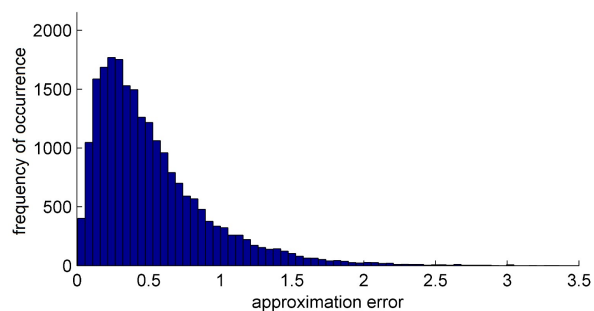
Fig. 10 Visualization of approximation errors for different compression ratios.

$$Errr = \frac{\sum_{i=1}^N \|\mathbf{v}_i - \bar{\mathbf{v}}_i\|}{N}, \quad (16)$$

where \mathbf{v}_i is the approximated vector, $\bar{\mathbf{v}}_i$ is the original vector and N is the number of vectors in the original dataset. This error shows how much the approximated vector field differs from the original one. The resulting error has the same units as the vector field. Next, we can compute another kind of



(a) Multilevel RBF approximation.



(b) Fourier approximation.

Fig. 11 Histograms of vector field approximation error for compression ratio 80 : 1.

approximation error. We can compute the average vector length error using the following formula

$$Err = \frac{\sum_{i=1}^N | \| \mathbf{v}_i \| - \| \bar{\mathbf{v}}_i \| |}{\sum_{i=1}^N \| \bar{\mathbf{v}}_i \|}. \quad (17)$$

This formula computes some kind of relative vector length error. The standard formula for relative vector length error is

$$Err = \frac{1}{N} \sum_{i=1}^N \frac{| \| \mathbf{v}_i \| - \| \bar{\mathbf{v}}_i \| |}{\| \bar{\mathbf{v}}_i \|}. \quad (18)$$

However, using this formula will give us incorrect result because of division by numbers close to zero or even equal to zero. For this reason we use (17) instead of the standard (18).

Last we will compute one more kind of approximation error, namely, the average angular displacement error. This error is computed using the following formula

$$Err = \frac{\sum_{i=1}^N \arccos \left(\frac{\mathbf{v}_i \cdot \bar{\mathbf{v}}_i}{\| \mathbf{v}_i \| \| \bar{\mathbf{v}}_i \|} \right)}{N}. \quad (19)$$

We compared our proposed method with the Fourier method using three types of approximation errors for different compression ratios. Computed approximation errors for our proposed multi-level vector field approximation and for the Fourier vector field approximation are visualized in Fig. 10. It can be seen, that for all three approximation errors computations, the proposed method has lower approximation error for all compression ratios. To analyze the approximation error more closely, we selected compression ratio 80 : 1 and computed histograms of approximation error using (13), see Fig. 11. It can be seen that most approximation errors are low and only a few errors are high.

Moreover to compare the two methods for vector field approximation, we computed the difference histogram, see Fig. 12. It can be seen, that the proposed method has much more lower approximation errors and much less higher approximation errors than the Fourier approximation method. The experiments made also proved similar behavior for other compression ratios.

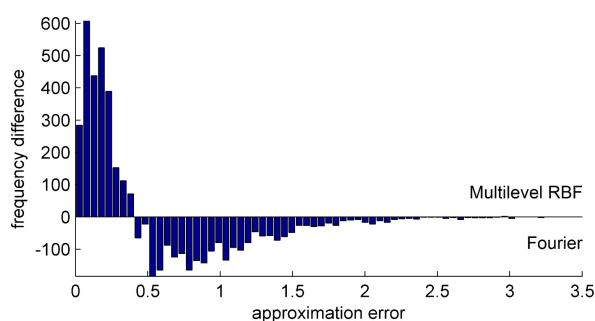


Fig. 12 Difference histograms of approximation errors (“Multilevel RBF” - “Fourier”), see Fig. 11, for compression ratio 80 : 1.

5 Conclusion

We proposed a new approach for multi-level vector field approximation. The vector field is approximated in several levels of details, where each level of details adds some additional information and refine the vector field approximation. The approach uses Radial basis function for approximation of vector field. The centers of radial basis functions are placed according to the distribution of approximation error of the previous level of detail vector field approximation. The proposed approach is especially convenient for approximation and visualization of large and complex data sets, i.e. only needed levels of details of the vector field can be transferred and visualized on the devices (mobile phone, web browser, etc.) with high compression ratio. Another advantage over existing approaches is the final analytical description of the approximated vector field, which can be used for further processing.

In the future, the proposed approach for multi-level vector field approximation will be extended to approximate the 3D vector fields as well. This extension should be straightforward and easy to implement.

Acknowledgment

The authors would like to thank their colleagues at the University of West Bohemia, Plzen, for their discussions and suggestions; colleagues at the Institute of Computer Science, the Czech Academy of Sciences, for their constructive comments and for providing testing data sets. The research was supported by projects Czech Science Foundation (GACR) No. GA 17-05534S and partially by SGS 2019-016.

References

1. Blazek, J.: Computational fluid dynamics: principles and applications. Butterworth-Heinemann (2015)
2. Bracewell, R.N., Bracewell, R.N.: The Fourier transform and its applications, vol. 31999. McGraw-Hill New York (1986)
3. Bülow, T., Felsberg, M., Sommer, G.: Non-commutative hypercomplex Fourier transforms of multidimensional signals. In: Geometric computing with Clifford algebras, pp. 187–207. Springer (2001)
4. Bürger, R., Ruiz, R., Schneider, K., Sepúlveda, M.A.: Fully adaptive multiresolution schemes for strongly degenerate parabolic equations with discontinuous flux. *Journal of Engineering Mathematics* **60**(3-4), 365–385 (2008)
5. Cabrera, D.A.C., Gonzalez-Casanova, P., Gout, C., Juárez, L.H., Reséndiz, L.R.: Vector field approximation using radial basis functions. *Journal of Computational and Applied Mathematics* **240**, 163–173 (2013)
6. Chung, E.T., Efendiev, Y., Lee, C.S.: Mixed generalized multiscale finite element methods and applications. *Multiscale Modeling & Simulation* **13**(1), 338–366 (2015)
7. Corbet, L., Vlček, O., Eben, K., Liczki, J., Benešová, N., Modlák, M.: Regional air quality forecasting for the Czech Republic. In: 15th International Conference on Harmonisation within Atmospheric Dispersion Modelling for Regulatory Purposes, HARMO 2013, pp. 150–154 (2013)
8. Davis, P.J.: Interpolation and approximation. Courier Corporation (1975)
9. Ebling, J., Scheuermann, G.: Clifford Fourier transform on vector fields. *IEEE Transactions on Visualization and Computer Graphics* **11**(4), 469–479 (2005)
10. Ell, T.A., Sangwine, S.J.: Hypercomplex Fourier transforms of color images. *IEEE Transactions on image processing* **16**(1), 22–35 (2007)
11. Fasshauer, G.E.: Meshfree approximation methods with MATLAB, vol. 6. World Scientific (2007)
12. Fourier, J.: *Theorie analytique de la chaleur*, par M. Fourier. Chez Firmin Didot, père et fils (1822)
13. Ghosh-Dastidar, S., Adeli, H., Dadmehr, N.: Principal component analysis-enhanced cosine radial basis function neural network for robust epilepsy and seizure detection. *IEEE Transactions on Biomedical Engineering* **55**(2), 512–518 (2008)
14. Günther, D., Jacobson, A., Reininghaus, J., Seidel, H.P., Sorkine-Hornung, O., Weinkauff, T.: Fast and memory-efficiently topological denoising of 2d and 3d scalar fields. *IEEE transactions on visualization and computer graphics* **20**(12), 2585–2594 (2014)
15. Helman, J., Hesselink, L.: Representation and display of vector field topology in fluid flow data sets. *IEEE Computer* **22**(8), 27–36 (1989)

16. Hitzer, E.M., Mawardi, B.: Clifford Fourier transform on multivector fields and uncertainty principles for dimensions $n=2 \pmod{4}$ and $n=3 \pmod{4}$. *Advances in Applied Clifford Algebras* **18**(3), 715–736 (2008)
17. Kansa, E.J.: Multiquadrics - A scattered data approximation scheme with applications to computational fluid-dynamics—i surface approximations and partial derivative estimates. *Computers & Mathematics with applications* **19**(8-9), 127–145 (1990)
18. Kansa, E.J.: Multiquadrics - A scattered data approximation scheme with applications to computational fluid-dynamics—ii solutions to parabolic, hyperbolic and elliptic partial differential equations. *Computers & mathematics with applications* **19**(8), 147–161 (1990)
19. Karim, A., Adeli, H.: Radial basis function neural network for work zone capacity and queue estimation. *Journal of Transportation Engineering* **129**(5), 494–503 (2003)
20. Kim, J.: Phase-field models for multi-component fluid flows. *Communications in Computational Physics* **12**(3), 613–661 (2012)
21. Koch, S., Kasten, J., Wiebel, A., Scheuermann, G., Hlawitschka, M.: 2d vector field approximation using linear neighborhoods. *The Visual Computer* **32**(12), 1563–1578 (2016)
22. Laramée, R.S., Hauser, H., Zhao, L., Post, F.H.: Topology-based flow visualization, the state of the art. In: *Topology-based methods in visualization*, pp. 1–19. Springer (2007)
23. Larsson, E., Fornberg, B.: A numerical study of some radial basis function based solution methods for elliptic PDEs. *Computers & Mathematics with Applications* **46**(5), 891–902 (2003)
24. Lee, H.G., Kim, J.: A comparison study of the boussinesq and the variable density models on buoyancy-driven flows. *Journal of Engineering Mathematics* **75**(1), 15–27 (2012)
25. de Leeuw, W., van Liere, R.: Multi-level topology for flow visualization. *Computers & Graphics* **24**(3), 325–331 (2000)
26. Majdisova, Z., Skala, V.: Big geo data surface approximation using radial basis functions: A comparative study. *Computers & Geosciences* **109**, 51–58 (2017)
27. Majdisova, Z., Skala, V.: Radial basis function approximations: Comparison and applications. *Applied Mathematical Modelling* **51**, 728–743 (2017)
28. Mohammadzade, H., Bruton, L.T.: A simultaneous div-curl 2d Clifford Fourier transform filter for enhancing vortices, sinks and sources in sampled 2d vector field images. In: *Circuits and Systems, 2007. ISCAS 2007. IEEE International Symposium on*, pp. 821–824. IEEE (2007)
29. Molina-Aiz, F., Fatnassi, H., Boulard, T., Roy, J., Valera, D.: Comparison of finite element and finite volume methods for simulation of natural ventilation in greenhouses. *Computers and electronics in agriculture* **72**(2), 69–86 (2010)
30. Pan, R., Skala, V.: A two-level approach to implicit surface modeling with compactly supported radial basis functions. *Engineering with Computers* **27**(3), 299–307 (2011)
31. Prakash, G., Kulkarni, M., Sripati, U.: Using RBF neural networks and Kullback-Leibler distance to classify channel models in free space optics. In: *Optical Engineering (ICOE), 2012 International Conference on*, pp. 1–6. IEEE (2012)
32. Reich, W., Scheuermann, G.: Analyzing real vector fields with clifford convolution and clifford-fourier transform. In: *Geometric Algebra Computing*, pp. 121–133. Springer (2010)
33. Rocha, H.: On the selection of the most adequate radial basis function. *Applied Mathematical Modelling* **33**(3), 1573–1583 (2009)
34. Schagen, I.P.: Interpolation in two dimensions - a new technique. *IMA Journal of Applied Mathematics* **23**(1), 53–59 (1979)
35. Skala, V.: Meshless interpolations for computer graphics, visualization and games. In: *Eurographics 2015 - Tutorials* (2015)
36. Skala, V.: High dimensional and large span data least square error: Numerical stability and conditionality. *International Journal of Applied Physics and Mathematics* **7**(3), 148–156 (2017)
37. Skala, V.: Least square method robustness of computations: What is not usually considered and taught. In: *Proceedings of the 2017 Federated Conference on Computer Science and Information Systems, Annals of Computer Science and Information Systems*, vol. 11, pp. 537–541. IEEE (2017)

38. Skala, V.: RBF interpolation with CSRBF of large data sets. *Procedia Computer Science* **108**, 2433–2437 (2017)
39. Skraba, P., Wang, B., Chen, G., Rosen, P.: 2d vector field simplification based on robustness. In: *Visualization Symposium (PacificVis)*, 2014 IEEE Pacific, pp. 49–56. IEEE (2014)
40. Smolik, M., Skala, V.: Vector field interpolation with radial basis functions. In: *Proceedings of SIGRAD 2016*, May 23rd and 24th, Visby, Sweden, 127, pp. 15–21. Linköping University Electronic Press (2016)
41. Smolik, M., Skala, V.: Spherical rbf vector field interpolation: experimental study. In: *Applied Machine Intelligence and Informatics (SAMi)*, 2017 IEEE 15th International Symposium on, pp. 431–434. IEEE (2017)
42. Smolik, M., Skala, V.: Vector field second order derivative approximation and geometrical characteristics. In: *International Conference on Computational Science and Its Applications*, pp. 148–158. Springer (2017)
43. Smolik, M., Skala, V., Majdisova, Z.: 3D vector field approximation and critical points reduction using radial basis functions. In: *International Conference on Applied Physics, System Science and Computers*, pp. 1–6. Springer (2018)
44. Smolik, M., Skala, V., Majdisova, Z.: Vector field radial basis function approximation. *Advances in Engineering Software* **123**, 117–129 (2018)
45. Smolik, M., Skala, V., Nedved, O.: A comparative study of lowess and rbf approximations for visualization. In: *International Conference on Computational Science and Its Applications*, pp. 405–419. Springer (2016)
46. Smolik Michal Skala, V.: Classification of critical points using a second order derivative. *Procedia Computer Science* **108**, 2373–2377 (2017)
47. Toivanen, J.I., Mäkinen, R.A., Haslinger, J.: Topology optimization in bernoulli free boundary problems. *Journal of Engineering Mathematics* **80**(1), 173–188 (2013)
48. Uhler, K., Skala, V.: Reconstruction of damaged images using radial basis functions. In: *Signal Processing Conference, 2005 13th European*, pp. 1–4. IEEE (2005)
49. Wendland, H.: Computational aspects of radial basis function approximation. *Studies in Computational Mathematics* **12**, 231–256 (2006)
50. Woollard, H., Billingham, J., Jensen, O., Lian, G.: A multi-scale model for solute transport in a wavy-walled channel. *Journal of Engineering Mathematics* **64**(1), 25 (2009)
51. Yingwei, L., Sundararajan, N., Saratchandran, P.: Performance evaluation of a sequential minimal radial basis function (RBF) neural network learning algorithm. *IEEE Transactions on neural networks* **9**(2), 308–318 (1998)
52. Zhang, X., Song, K.Z., Lu, M.W., Liu, X.: Meshless methods based on collocation with radial basis functions. *Computational mechanics* **26**(4), 333–343 (2000)